COMPUTER METHODS AND PROGRAMS IN BIOMEDICINE 108 (2012) 28–37

journal homepage: www.intl.elsevierhealth.com/journals/cmpb

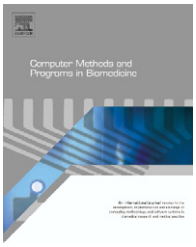

Transformation of videocapsule images to detect small bowel mucosal differences in celiac versus control patients

Edward J. Ciaccio[a,*], *Christina A. Tennyson*[a], *Govind Bhagat*[a,b], *Suzanne K. Lewis*[a], *Peter H.R. Green*[a]

[a] *Department of Medicine, Columbia University Medical Center, 180 Fort Washington Avenue, New York, NY 10032, USA*
[b] *Department of Pathology and Cell Biology, Columbia University Medical Center, 180 Fort Washington Avenue, New York, NY 10032, USA*

ARTICLE INFO

Article history:
Received 24 March 2011
Received in revised form
16 October 2011
Accepted 13 December 2011

Keywords:
Celiac disease
Ensemble average
Spectral analysis
Videocapsule imaging
Villous atrophy

ABSTRACT

Background: Videocapsule endoscopy can be useful to detect small intestinal pathology in celiac disease patients. However, presence of extraneous features including air bubbles and opaque fluids can complicate the analysis. A technique for quantitative analysis of videocapsule images is presented that is robust to presence of extraneous features.
Method: Videocapsule clips were acquired from five small intestinal locations in 12 celiacs with villous atrophy and 11 control patients. Clips were 200 frames in length, their resolution was 576×576 pixels and 256 grayscale levels, with 2/s frame rate. The dominant period (DP), defined as the tallest peak in the ensemble average power spectrum, was computed over each clip without removal of extraneous features. Ensemble average basis images were constructed, and measurements were made of their frame-to-frame variation in brightness and texture.
Results: From pooled basis images, celiac images had greater texture than controls and exhibited more brightness variation ($p < 0.05$ in mean and $p < 0.01$ in standard deviation). In celiacs, correlation existed between greater textural alterations versus longer DP ($r^2 = 0.47$), and between greater brightness variation and longer DP ($r^2 = 0.33$). There was no significant correlation between quantitative features and DP in controls ($r^2 < 0.25$).
Conclusions: Using this new method, celiac videoclips were quantitatively distinguishable from control videoclips without manual or computer-assisted detection, masking, and removal of extraneous image features. Furthermore, in celiac but not control basis images, larger textural and brightness alterations were correlated to longer DP. Greater textural and brightness alterations, and thus longer periodicities, are likely related to presence of villous atrophy.

1. Background

Celiac disease is present in 1% of the population, worldwide and is caused by an autoimmune reaction to dietary gluten [1]. A major clinical manifestation of celiac disease is the presence of villous atrophy in the small intestinal mucosa, which prevents normal absorption of nutrients from food [2,3]. Serological testing for antibodies to tissue transglutaminase is usually the first step in the diagnosis of celiac disease,

* *Corresponding author at*: Harkness Pavilion 804, Columbia University, 180 Fort Washington Avenue, New York, NY 10032, USA. Tel.: +1 212 305 5447; fax: +1 212 342 0447.
E-mail address: ejc6@columbia.edu (E.J. Ciaccio).
0169-2607/$ – see front matter © 2011 Elsevier Ireland Ltd. All rights reserved.
doi:10.1016/j.cmpb.2011.12.008

followed by conventional upper gastrointestinal endoscopy with duodenal biopsy which is the current the gold standard [3–5]. Conventional endoscopy is invasive and is limited to study of proximal areas of the small intestine. There is the possibility that mucosal pathology may be present in the more distal small intestine, which is not accessible during routine endoscopy. Conventional endoscopy requires sedation and depends on patient willingness to undergo this procedure. Small bowel biopsies obtained during endoscopy have limitations. Regions of patchy villous atrophy may be missed and the tissue may not be adequately oriented [6,7]. By comparison, videocapsule endoscopy, which was introduced clinically in 2001 [4,8], enables the examination of the entire small bowel with visualization of mucosal villi. The imaging device consists of a white-light disposable capsule which is swallowed by the patient with water after overnight fasting. Peristalsis moves the capsule through the gastrointestinal tract. Since its inception, videocapsule endoscopy has increasingly become an important diagnostic tool for examining the small intestine [9,10]. The procedure is essentially noninvasive and has sufficient sensitivity to be useful for the detection of small bowel bleeding, tumors, damage caused by nonsteroidal anti-inflammatory drugs (NSAIDs), and Crohn's disease, in addition to celiac disease.

Videocapsule endoscopy has good sensitivity and excellent specificity for the detection of villous atrophy in patients with suspected celiac disease [4]. Capsule endoscopy findings in untreated celiac disease patients include villous atrophy (68%), fissuring (62%), layering (40%), and mosaic patterns (19%) [7]. Capsule endoscopy interpretation is subjective. Quantitative analysis of videocapsule data by computational means, using methodology that compresses the data to salient features, followed by measurement of the statistical properties in the compressed images, can be used for improved detection and measurement of the small bowel manifestation of celiac disease. Quantitative analysis may be difficult when artifacts such as air bubbles or luminal fluid are present. In this study, a method to transform videocapsule imaging data for retention of salient information is described that is robust to the presence of extraneous features including air bubbles and opaque fluids. This method is used for quantitative analysis of successive videocapsule image frames to extract relevant features. Images from celiacs having small intestinal villous atrophy, versus controls lacking atrophy, can be quantitatively compared.

2. Methods

2.1. *Clinical procedure and data acquisition*

All patients were evaluated at Columbia University Medical Center, New York, from May 1, 2008 to July 31, 2010. Retrospective videocapsule endoscopy data was obtained from twelve celiac patients. In these patients the diagnostic biopsy showed Marsh grade II–IIIC lesions. Retrospective videocapsule endoscopy data was also obtained from eleven control patients who did not have celiac disease. Informed consent was obtained from all patients prior to videocapsule endoscopy. Indications for this procedure included suspected celiac disease, suspected Crohn's disease, obscure bleeding, iron deficient anemia, and chronic diarrhea. All the patients from which celiac data was acquired had biopsy-proven celiac disease, except for one patient with hemophilia who did not have a biopsy but was positive for anti-endomysial and tissue transglutaminase antibodies. These patients were being additionally evaluated by videocapsule endoscopy because they were considered to have complicated celiac disease including abdominal pain that was unexplained by previous evaluation. Exclusion criteria for this study included patients under 18 years of age, those with a history of or suspected small bowel obstruction, dysphagia, presence of pacemaker or other electromedical implants, previous gastric or bowel surgery, and, pregnancy. Only complete videocapsule endoscopy studies, reaching the colon, were used for analysis. The retrospective analysis of videocapsule endoscopy data was approved by the Internal Review Board at Columbia University Medical Center.

The PillCamSB2 videocapsule (Given Imaging, Yoqneam, Israel) was utilized to obtain the small bowel images in the study groups. The system consists of a recorder unit with cradle, real-time viewer and cable, battery pack, antenna lead set, recorder unit harness, and battery charger. The capsule weighs 3.7 g, its dimensions are 26 mm × 11 mm, and it acquires two digital frames per second. It is a single-use pill-size device, which is swallowed and passes naturally through the gastrointestinal tract [11]. The PillCam has three components: the capsule or mini-endoscope, an external receiving antenna with hard-drive for data storage, and a HIPAA-compliant PC console with dedicated software for image analysis. Image features include a 140° field of view, 1:8 magnification, 1.30 mm depth of view, and a resolving power of approximately 0.1 mm. The activated capsule provides images until the battery expires, usually 8 h. Thus it acquires up to 55,000 images.

For each patient undergoing the procedure, eight abdominal leads were placed in the upper, mid, and lower abdomen. A belt containing the data recorder and battery pack was affixed around the waist. All subjects swallowed the PillCam SB2 in early morning with approximately 200 cm^3 of water and 80 mg simethicone, after a 12 h fast without bowel preparation. Subjects were allowed to drink water 2 h after ingesting the capsule, and to eat a light meal after 4 h. The recorder received radioed images from the videocapsule as it passed through the GI tract. The investigation was terminated either after 8 h or when the battery life expired. The belt data recorder was then removed, and the data was downloaded to the dedicated computer console. Videos were reviewed, interpreted, and exported for further analysis by an experienced gastroenterologist using Given Imaging analysis software. De-identified video clips of 200 frames acquired from five locations in the small intestine of each patient were obtained and analyzed retrospectively. Images were acquired immediately distal to the pylorus corresponding to the proximal duodenum and immediately proximal to the colon, corresponding to the distal ileum (locations 1 and 5, respectively). The total small bowel transit time of the video capsule was divided into tertiles. Video clips were also acquired from each of the three tertiles for each patient (locations 2–4).

The retrospectively obtained patient videoclips were then transferred to a dedicated PC-type computer for development of features for quantitative analysis. Each RGB color videoclip

was first converted to a series of grayscale images (256 brightness levels, 0 = black, 255 = white) with an image resolution of 576 × 576 pixels, using Matlab Ver. 7.7, 2008 (Mathworks, Natick, MA). Both celiac and control patients were found to have opaque intraluminal fluid and air bubbles in portions of the image frames. These materials were sometimes present in all of the videoclip images and covered substantial portions of each frame. For purposes of quantitation, as a first approximation the extraneous features were considered to act as random noise on the quantitation process, which is described below. To test the robustness of the method, all videocapsule images were quantified—none were excluded regardless of the presence of extraneous material in the images.

2.2. *Spectral analysis and transformation*

2.2.1. *Dominant period analysis*

To estimate wall motion, the dominant period of image grayscale value was calculated over 200 frames using the ensemble average method [12,13]. Briefly, the ensemble average vector $\underline{\mathbf{e}}_w$ is obtained by averaging successive mean-zero signal segments of window length w:

$$\underline{\mathbf{e}}_w = \frac{1}{n} \cdot \mathbf{U}_w \cdot \underline{x} \tag{1a}$$

$$\mathbf{U}_w = [\mathbf{I}_w \mathbf{I}_w \ldots \mathbf{I}_w] \tag{1b}$$

where $\underline{x}$ is the length N signal vector, the computation matrix $\mathbf{U}_w$ is $w \times N$ in dimension, and $\mathbf{I}_w$ are $w \times w$ identity submatrices used to form the signal segments that are extracted from $\underline{x}$ and summed. The number of summed signal segments of length w is:

$$n = \text{int}\left(\frac{N}{w}\right) \tag{2}$$

The ensemble average power is given by:

$$P_w = \frac{1}{w} \underline{\mathbf{e}}_w^T \cdot \underline{\mathbf{e}}_w \tag{3}$$

To generate an ensemble average power spectrum, the root mean square (RMS) power is used [12,13]:

$$P_{\text{wRMS}} = \sqrt{P_w} \tag{4}$$

with units of mV. The frequency spectrum is then formed by plotting $\sqrt{n} \times P_{\text{wRMS}}$ versus w with the $\sqrt{n}$ term being used to eliminate the effects of ensemble averaging on the noise floor level. Based on the 200 frame videoclips that were extracted for analysis, the low spectral limit was selected as 40 frames (20 s), and the high spectral limit was 3 frames (1.5 s). The dominant frequency (DF) was defined as the tallest fundamental peak in the ensemble average power spectrum [14], which was converted to dominant period (DP) by:

$$\text{DP} = \frac{\text{sampling rate}}{\text{DF}} = \frac{(2/\text{s})}{\text{DF}} \tag{5}$$

Calculation is straightforward for a mean-zero biomedical signal $\underline{x}$ [12,13]. For image quantitation, in previous work [14] the elements of vector $\underline{\mathbf{x}}$ were the average brightness x_i of the image frames for i = 1–200. While this method proved helpful to discern celiac from control videoclips using a three-dimensional classification system (dominant period, texture, and brightness), it is based on limited information since it is computed from average data. In the present study, the ensemble average power spectrum was computed for each pixel j:

$$P_w(j) = \frac{1}{w} \underline{\mathbf{e}}_w(j)^T \cdot \underline{\mathbf{e}}_w(j) \tag{6}$$

$$P_{\text{wRMS}}(j) = \text{sqrt}\left[\frac{P_w(j)}{w}\right] \tag{7}$$

The power for all pixels over the video image sequence is then calculated as:

$$P_{\text{w\_clip}} = \frac{1}{N^2} \sum_j P_{\text{wRMS}}(j) \tag{8}$$

where $N \times N$ is the image dimension (576 × 576). $P_{\text{w\_clip}}$ was then plotted versus w to form the power spectrum.

To represent salient information, videos can be approximated by a series of basis images [15]. In the present study, basis images were constructed from the ensemble averages of image frames using the DP for determining which frames to add. For example, suppose the DP = 5 s, which means that the dominant periodicity occurs every 10 image frames when the frame rate is 2/s. The ten 576 × 576 element basis images $\mathbf{B}$ are computed from the 576 × 576 element image frames $\mathbf{F}$ as:

$$\begin{aligned} \mathbf{B}_1 &= (1/20) \quad \mathbf{F}_1 + \mathbf{F}_{11} + \ldots + \mathbf{F}_{191} \\ \mathbf{B}_2 &= (1/20) \quad \mathbf{F}_2 + \mathbf{F}_{12} + \ldots + \mathbf{F}_{192} \\ &\vdots \\ \mathbf{B}_{10} &= (1/20) \quad \mathbf{F}_{10} + \mathbf{F}_{20} + \ldots \mathbf{F}_{200} \end{aligned} \tag{9}$$

The basis images were then used for quantitation. Brightness variability among the basis images was measured as the standard deviation in mean brightness level of 10 × 10 subimages, averaged for 57 × 57 subimages in each $\mathbf{B}_k$, excluding edge elements [14,16]. Image texture was measured by taking the square root of the sum of squares difference from the mean in each 10 × 10 subimage, and averaging for 57 × 57 subimages in each $\mathbf{B}_k$, excluding edge elements [14,16]. The image texture variability was the standard deviation from the mean image texture. The DP, brightness variability, and image texture and its variability were tabulated and separately pooled for celiac and for control patient videoclips.

As an additional measure of texture, the basis images were transformed into edge-detected images using ImageJ, a public domain Java image processing program (Ver. 1.43u, National Institutes of Health, Bethesda, MD). The edge-detected images were then binarized. The mean number and size of discrete edges in the binarized images were computed using ImageJ and compared for celiacs versus controls.

For all calculations, the unpaired t-test was used to determine the statistical significance between mean values and the f-test was used to detect differences between standard deviations. Using a small sample of celiac and control videoclips for estimation, the mean number of distinct edges in binarized basis images had an average difference of approximately

900 ± 1200. We determined the required sample size as follows. The power test is used to determine the probability of detecting a difference between groups (SigmaPlot ver. 9.01, 2004, Systat Software Inc.). A power of 0.80 is desirable, meaning an 80% chance of detecting an effect with 95% confidence when $\alpha = 0.05$. Based on this test, the power P would be 0.4 if 11 control and 12 celiac patient videoclips were used for analysis. To attain a power of 0.8, 30 control and 30 celiac patients would be needed. To ensure significance, we pooled videoclip data from the five locations in 11 celiacs and 10 controls (respectively, $N = 55$ and $N = 50$) for statistical analysis.

Best subsets correlation was used to determine correspondence between the DP and the quantitative image features (brightness and texture variations). Statistical comparisons were done using SigmaPlot 2004 for Windows Version 9.01 (Systat Software, Inc.) and MedCalc 2010 Ver. 11.4 (MedCalc Statistical Software) with significance at $p < 0.05$ for the t-test and f-test, and $r^2 > 0.25$ for correlation tests.

3. Results

Celiac images often appeared distinctive by eye as compared to control images obtained from the videoclips. The intestinal mucosa in control images generally consisted of regular folds and uniform, lightly textured surfaces as shown in Fig. 1A and B (some opaque fluid can be observed at the center of 1B). The entire appearance of each image thus was generally one of homogeneity for the control patients although presence of extraneous features added a random component to the data. In contrast, heterogeneity was often present in celiac patient images as in Fig. 1C and D. For example there is fissuring in the mucosal surface shown in Fig. 1C, and scalloping of the edges of mucosal folds were often apparent in celiac images as in Fig. 1D. Overall, there was visual evidence of a greater variability in texture, contrast, and gross features in celiac images as compared with controls in the videoclips at all five small intestinal locations analyzed for this study.

Differences in celiac versus control videoclips were manifested in the DP basis images as is shown in an example in Fig. 2. In panel A are basis images constructed from a control image series, while panel B shows basis images from a celiac image series. All basis images shown were constructed from videoclips acquired at location 2 (distal duodenum). For Fig. 2, the DP was 5.5 s (11 basis images) in controls and 8.5 s (17 basis images) in celiacs. Shown are four basis images from each set. The control basis images (Fig. 2A) have the general appearance of relative smoothness and homogeneity in brightness, contrast, and features. Although a few dark areas are evident toward the center in each panel, which are manifestations of the camera angle directed toward the center of the intestinal lumen at depth, these markings are subtle. By comparison, there are relatively sharp features and more heterogeneity in the celiac basis images (Fig. 2B). Very bright and very dark areas are evident as in the first celiac basis image at left. There is a relatively high degree of fissuring evident in all of the celiac basis images (lines). These fissures partially subdivide each basis image according to differing textural properties. Individual features vary greatly and include isolated black and white structures.

A close-up of a control basis image from the series with enhanced processing is shown in Fig. 3. In panel A is the unprocessed basis image. In panel B the contrast is enhanced using ImageJ. In panel C the edges are detected, also using ImageJ. In panel D the binarized image derived from the edge-detected image via ImageJ is shown. Even with the enhanced processing (panel D), there is still the appearance of relative uniformity in this control basis image. Except for the slightly darker region at center, the texturally derived properties appear to be mostly constant, with slight variation in gray shading (panels A and B). The edge detection image, in terms of density and characteristics of edges, are also mostly uniform (curved lines, panels C and D). By comparison, a close-up of a celiac basis image is shown in Fig. 4, with the same processing in each panel as was described for Fig. 3. There are marked changes in brightness and texture in the original and in the contrast-enhanced image (Fig. 4A and B). The textural properties appear to vary greatly over the spatial extent of the basis image, ranging from smooth and white (center-right in panel B), to mottled (top and bottom in panel B), to isolated dark structures (left in panel B). The edges (Fig. 4C) show highly varying length, thickness, and degree of curvature as compared to the edge detection basis image of the control patient (Fig. 3C). Fused structures appear at several locations (Fig. 4C). The binary edge-detection image is heterogeneous (Fig. 4D), showing fewer but longer and less uniform edges that are interspersed with large blank areas as compared with Fig. 3D.

3.1. *Quantitative comparison*

Summary quantitative statistics for textural properties of the DP basis images are shown in Table 1. The brightness variability ($p < 0.05$) and image texture (NS) and its variability ($p < 0.05$) were larger in celiacs as compared with controls. Furthermore, the standard deviations in brightness and image texture variability, and the DP, were all significantly greater in celiacs as compared with controls, indicating more frame-to-frame variability in celiacs. The DP was longer in celiacs as compared with control patients (NS in this series). These values and significances differ from those presented in an earlier work [14] due to the fact that in the present study, basis images were used rather than the original images, while extraneous features including air bubbles and opaque fluids were not removed. Thus it is possible to detect and evaluate quantitative differences in celiac versus control videoclips without preprocessing the image frames for removal of extraneous features.

Ensemble spectra were created for celiac and control images at each of the five small intestinal locations. An example is shown in Fig. 5 for data obtained from locations 3 to 4 in selected patients. Spectra were constructed with period (=1/frequency) along the x-axis. Prominent peaks are labeled as fundamental frequency (labeled 1) and harmonics. For the control patient, the DP occurs between 4 and 5.5 s, while for the celiac patient, the DP occurs between 6 and 9 s. Thus at these particular locations in the small bowel, frame-to-frame periodicity is longer in the celiac patient as compared with the control patient, in agreement with Table 1.

Tables 2a and 2b show how best subsets linear correlation was used to estimate dependencies between the DP and

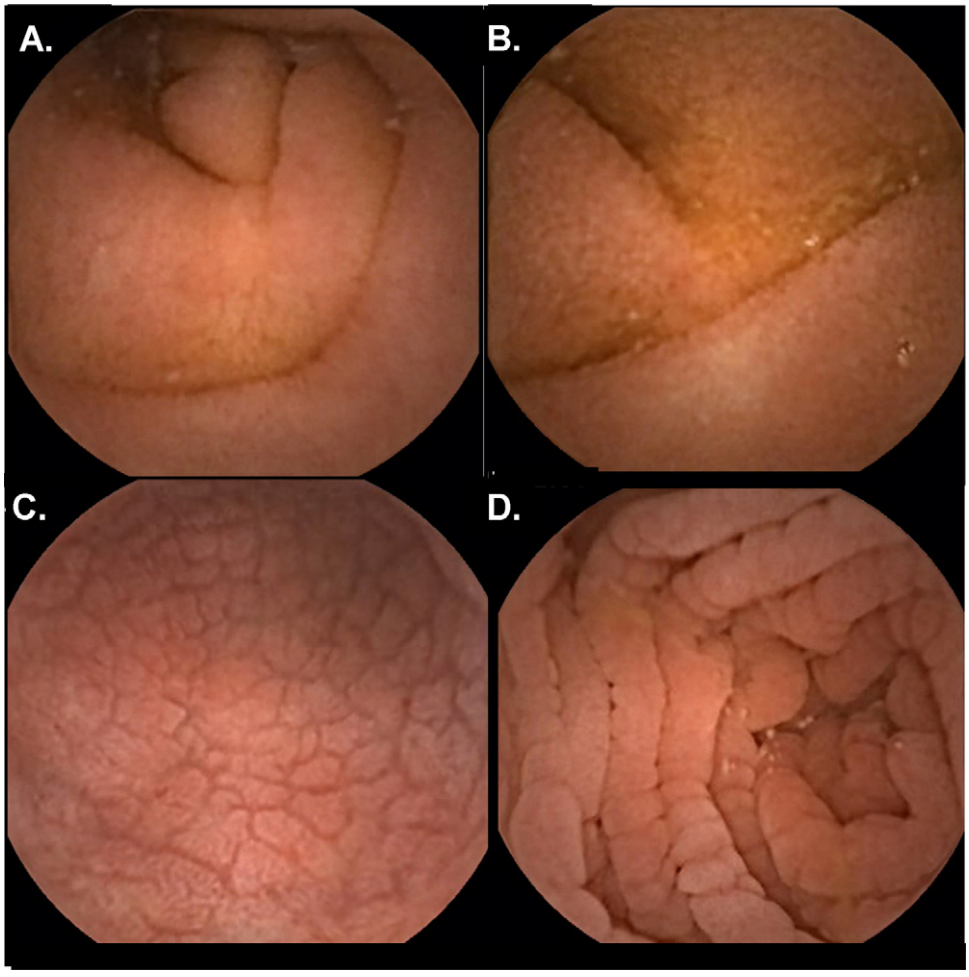

Fig. 1 – Example of videocapsule images from the distal duodenum of a control (A and B) and celiac (C and D) patient. There is layering of folds in the celiac case (panel D). In panels C and D, the texture and brightness of each surface vary over both small and large distances, including graininess and degree of coarseness along the surface, as compared with the greater homogeneity and smoother texture evident in control images (A and B).

the brightness and texture features. In control patients, the brightness variation is best correlated to DP, yet the correlation coefficient is only 0.21. Even when a second and the third feature are added to the correlation model, r^2 only increases to 0.24. When texture and its variability were correlated to DP without brightness variation included, r^2 was found to be 0.14 (not shown). Thus there is minimal linear correlation between the DP and textural properties in control image frames. By comparison, in celiac patients, there is a relatively strong correlation of texture variability to DP ($r^2 = 0.47$ and 0.54 for models 1 and 2). Yet, addition of the brightness variability as a third feature did not significantly increase the correlation to DP ($r^2 = 0.55$). When brightness variability was correlated to DP without texture included, $r^2 = 0.33$ (not shown). Thus overall, there is substantial and linear correlation of texture, and to a lesser extend brightness variability, to the DP in celiacs but not in controls.

In Fig. 6, a three-dimensional scatterplot is shown for pooled control ($N = 5 \times 11 = 55$) and celiac patients ($N = 5 \times 12 = 60$). Feature axes are shown, and colors of

Table 1 – Summary of capsule quantitative measurements.

Feature	Celiacs ($N = 12$)	Controls ($N = 11$)	t-Test	f-Test
Brightness variability (gsl)	4.79 ± 2.43	4.05 ± 1.72	$p < 0.05$	$p < 0.01$
Image texture (gsl)	5.62 ± 3.61	5.48 ± 3.63	NS	NS
Image texture variability (gsl)	0.43 ± 0.47	0.29 ± 0.25	$p < 0.05$	$p < 0.001$
Dominant period (s)	7.57 ± 3.55	7.17 ± 2.74	NS	$p < 0.05$

Data is shown as mean ± standard deviation; t-test, significance of the difference in the means based on the unpaired t-test; f-test, significance of the difference in the variances based on this test. NS = not significant, gsl = grayscale level.

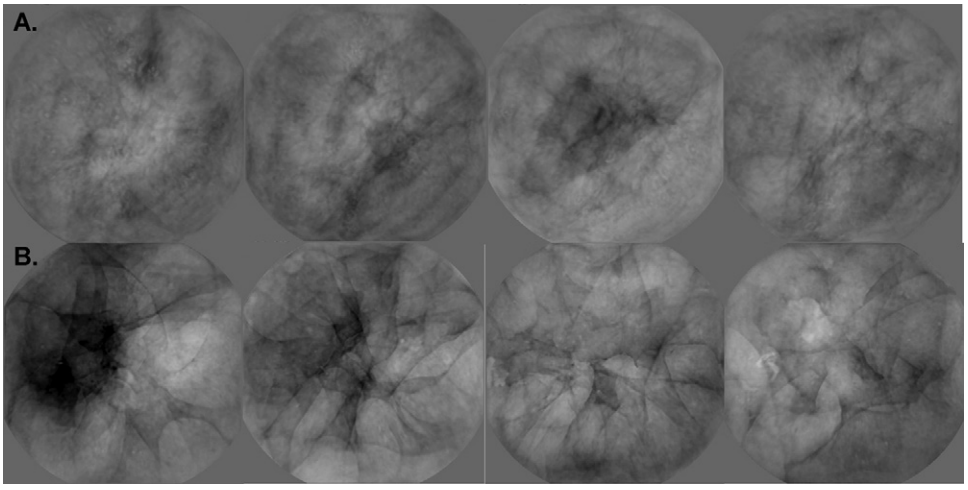

Fig. 2 – Mosaic of four selected basis images from a control patient (A) and a celiac patient (B) from the same sequences as were used to construct Fig. 1. The control patient basis images (A) appear smoother with few if any crevasses, scalloping, and fissures as compared with the celiac images (B). There is a greater spatial regularity to the control patient texture (A). The slightly dark area toward the center in (A) is caused by the videocamera pointing toward the lumen center at depth in some frames, which is not entirely brightened by the PillCam. The celiac images (B) contain a greater variety of brightness and textural singularities, as well as sharp crevasses and fissures.

Table 2a – Correlation of dominant period to other features—controls.

Controls	Feature	Slope	Significance	r^2
Model # 1	Brightness var	0.72	$p < 0.001$	0.21
Model # 2	Brightness var	0.68	$p = 0.001$	0.24
–	Texture	0.14	NS	–
Model # 3	Brightness var	0.79	$p = 0.017$	0.24
–	Texture	0.13	NS	–
–	Texture var	−0.99	NS	–

var = variability; Slope, slope of the linear regression line. A positive slope indicates a direct correlation between variables, negative slope indicates inverse correlation between variables.

points denote their DP as defined by the scale. The feature magnitudes mostly diminish with decreasing DP (more dark blue points at upper left), in agreement with Tables 2a and 2b. When control and celiac data from all five locations was pooled, there was a positive correlation between texture and DP ($r^2 = 0.69$, $p < 0.02$). Thus sequences with greater texture also tended to have longer DP, in agreement with Tables 2a and 2b.

Table 2b – Correlation of dominant period to other features—celiacs.

Celiacs	Feature	Slope	Significance	r^2
Model # 1	Texture var	5.19	$p < 0.001$	0.47
Model # 2	Texture	0.29	$p = 0.004$	0.54
–	Texture var	4.26	$p < 0.001$	–
Model # 3	Brightness var	−0.25	NS	0.55
–	Texture	0.30	$p = 0.004$	–
–	Texture var	5.40	$p < 0.001$	–

var = variability; Slope, slope of the linear regression line. A positive slope indicates a direct correlation between variables, negative slope indicates inverse correlation between variables.

3.2. *Edge detection and measurement*

Using ImageJ, the mean number of distinct edges in the binarized basis images was 1603.07 ± 736.03 for celiacs versus 2511.47 ± 1116.57 for controls ($p < 0.001$). The mean edge size was 34.26 ± 20.17 for celiacs versus 29.03 ± 12.00 for controls ($p = 0.003$). Thus there were decreased but larger edges in celiacs, as might be caused by fissuring and scalloping (see Fig. 1C and D), and these were interspersed with smoother areas lacking pronounced edges, as would be expected when patchy villous atrophy is present. In control basis images there were more but smaller edges, which were more uniformly distributed, as would be anticipated in the case of a normal villous architecture.

4. Discussion

4.1. *Summary*

In this study 200 frame videocapsule images were analyzed without detection and removal of frames and image areas having artifacts such as air bubbles and opaque fluids. For robust quantitative analysis, these features were transformed so that salient information was retained while extraneous features acting as random components were removed. It was found that celiac image frames have textural properties of greater magnitude (mean) and variability (standard deviation) as compared with controls (Table 1). It was found by quantitating the basis images that in celiacs, when texture is greater, as might be caused by increasing levels of villous atrophy, the DP lengthens as might be related to lesser gastrointestinal motility due to the injury (Tables 2a and 2b). These are unique findings

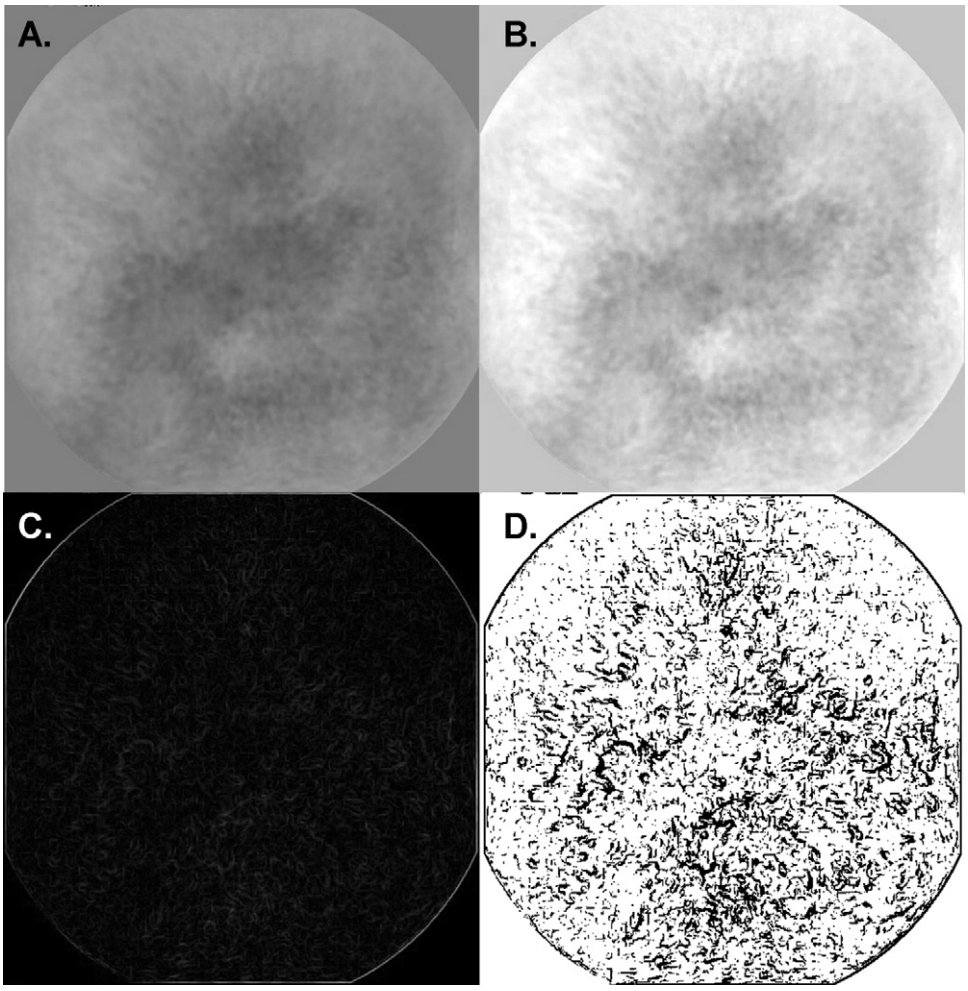

Fig. 3 – Close-up of a basis image from the control patient image, with differential processing: (A) the original basis image; (B) the contrast-enhanced image; (C) image with edge detection; (D) binarized edge detection image.

that were determined via the use of basis images, which are automatically computed without manual intervention, and eliminate the need for extraneous noise removal. The lack of a noise removal preprocessing step is important for the analysis paradigm and can increase speed of computation over many image frames, which will become important as higher resolution capsule videocameras become available as well as when longer videoclips or entire videos of the small intestine are analyzed. The possibility that peristalsis and other characteristics of gastrointestinal motility may be related to the level of villous atrophy in celiacs is intriguing and merits further study. If it can be shown that defects in gastrointestinal motility are related to presence of villous atrophy, or vice versa, it could represent a major advance in addressing the mechanism by which patch villous atrophy forms and changes in celiac patients.

4.2. *Image analysis and representation of the mucosal architecture*

For simplicity the degree of light exposure and depth were not considered in our calculations; thus the automated PillCam features were useful to provide homogeneity of image quality and brightness [10]. The dominant period averaged 7.17 ± 2.74 s in control patients (14.34 basis image frames) and 7.57 ± 3.55 s in celiacs (15.14 basis images frames) (Table 1). The dominant period, as described in the Methods, is the fundamental periodicity in the frame-to-frame videocapsule image sequence. This represents a reduction to a compression ratio of ~200/15 = 13:1. Although only one frequency component – the DP – are encoded in the basis images that were used in the study, these basis images were found useful for estimation of quantitative differences in celiac versus control patient videoclips. This is due to the fact that the DP contains the largest correlated content while ignoring transients and other noise; for example, the extraneous materials present in the images. By including additional basis images in the reconstruction in future studies, for example by including nonharmonic peaks with large spectral power (as at ~10 Hz in Fig. 5B), discrimination of celiac versus control images based on textural differences is potentially improved, subject of future study.

Texture was also represented by the number and size of discrete edges in the basis images, as measured by ImageJ. These edges were representative of the luminal architectural profile. If the lumen is homogeneous, as would be anticipated in control patients with normal villi, many minute discrete

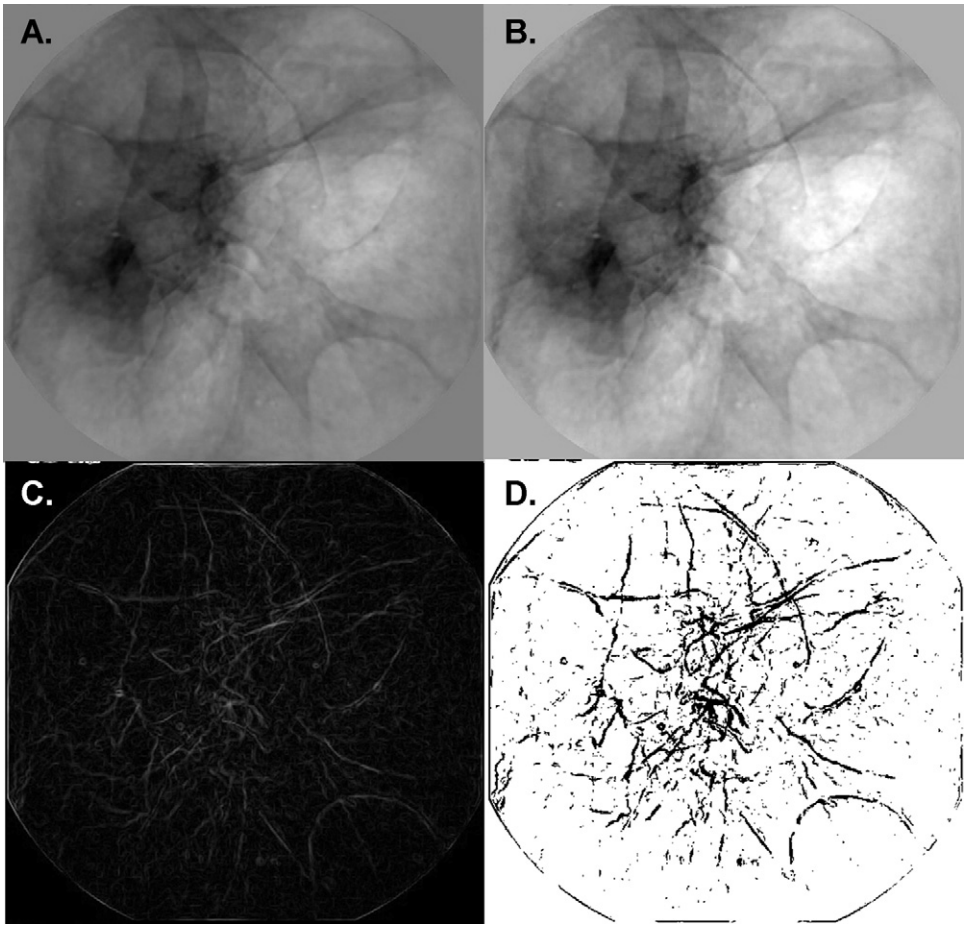

Fig. 4 – Close-up of a basis image from the celiac patient image with differential processing. The differential processing is the same as in corresponding panels of Fig. 3.

edges should be present, as was actually observed (see Section 3). In celiac patients with pathology, patchy villous atrophy is present, causing varying degrees of villous projection, or no projection, from the luminal surfaces, as well as larger anatomic abnormalities including fissuring and mosaic pattern. Thus lesser discrete edges of longer length would be expected and was observed (see Section 3).

4.3. *Clinical correlates*

Most untreated celiac patients undergoing videocapsule endoscopy have visible atrophy [9,17] that is patchy [1,3,5]. Only approximately half of celiac patients exhibit extensive enteropathy, with about one third having enteropathy limited to the duodenum. As compared with standard endoscopy, coverage is throughout the small intestine rather than being constrained to the duodenum [9,17]. Because of the magnification of videocapsule images, villous architecture may be better appreciated as compared with images obtained during standard endoscopic examination. Detection of villous atrophy from the capsule endoscopy images is therefore often possible when assessment is done by an expert gastroenterologist. Use of computerized methods to analyze videocapsule images can further improve sensitivity, owing to the possibility of detecting low-level atrophy that would be missed by visual inspection. Prior methodology has shown that three quantitative measures of image brightness and texture can be used to distinguish celiac versus control small intestinal mucosa when videoclips of length equal to 200 image frames (duration of 100 s) are processed [14,16]. Presumably, this ability to discern celiacs versus controls is due to the presence of villous atrophy in the celiacs, which is manifested as greater image texture and greater textural variation. In the current study, we showed that the magnitude of brightness and textural features is proportional to the dominant period in data pooled from celiacs and controls combined (Fig. 6). Separately, the celiac patients tended to have greater correlation of texture to DP while control patients had substantially less correlation (Tables 2a and 2b), perhaps owing to greater homogeneity and lesser degree of texture in the control images (Fig. 3, Table 1). Texture is a spatial variable and is equivalent to the spatial variation in pixel brightness. In celiacs, where texture is greater, as might be caused by villous atrophy of varying degrees, DP is longer, as may be related to decreased gastrointestinal motility due to the injury. However, this supposition should be examined in a future series of patients with biopsy-proven villous atrophy. The greater texture magnitude in celiac patients (Table 1) is likely related to presence of villous atrophy. The longer DP found in celiac patients (Table 1), which was correlated to textural properties (Fig. 6) may be directly

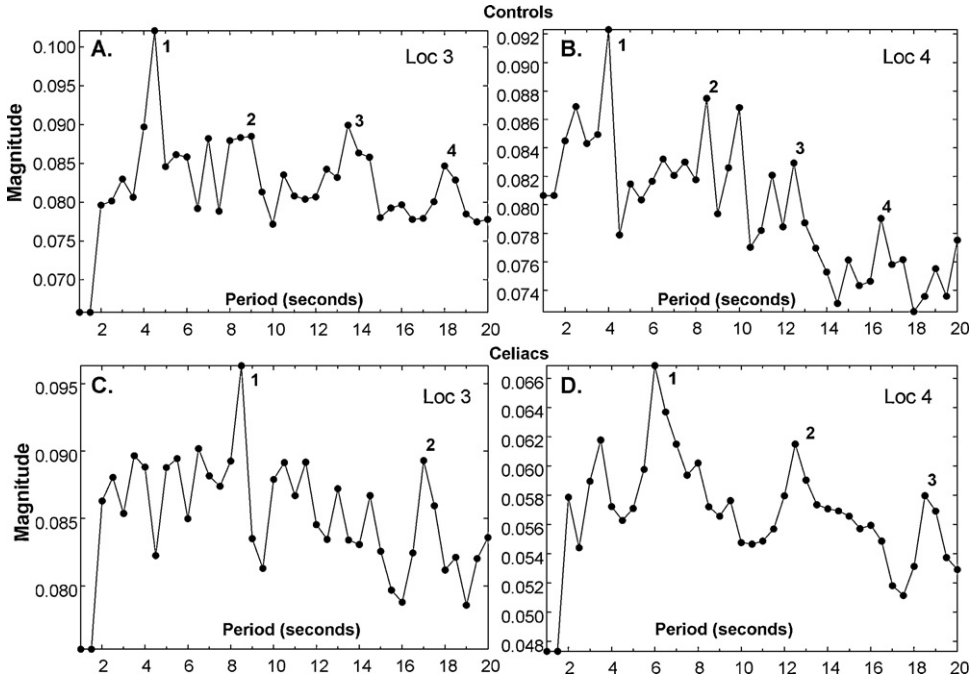

Fig. 5 – Frequency spectrum at locations 3 and 4 (jejunum—proximal ileum). Dominant period and harmonics are shown: (A and B) control patient—DP is relatively short; (C and D) celiac patient—DP is relatively long.

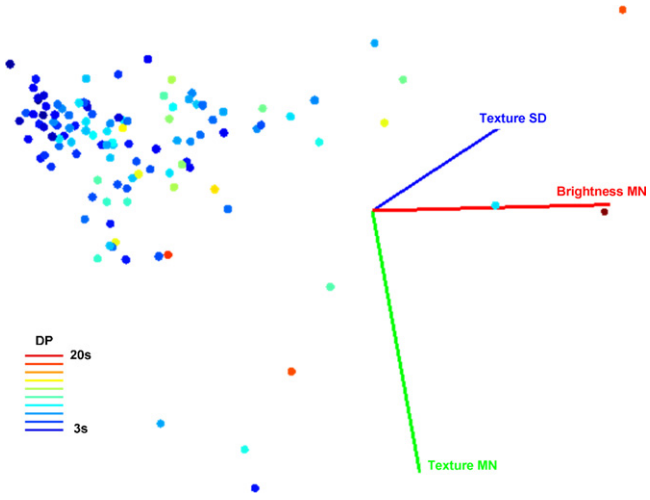

Fig. 6 – Relationship between feature variables and dominant period DP. As DP lengthens from blue to red, the magnitude of feature variables tends to increase. The zero value for all features is at the vertex of the conical distribution formed by the set of points (toward upper left).

related to abnormal small intestinal motility [18] although this hypothesis must be tested in future work.

On a long term gluten-free diet, the extent and pattern of atrophy improves both qualitatively and quantitatively [3,17]; so that detection of any lingering pathology in endoscopy images becomes more difficult. However, even the presence of very mild or subtle pathology is more likely to be evident when using computerized methods of image analysis since the slightest differences in gray (or color) level can be discerned. No association has been shown between the extent of small intestinal mucosal lesions caused by villous atrophy and clinical manifestations of celiac disease [1,2,5]. Hence regardless of the treatment state of celiac patients, there is unlikely to be a high degree of correlation between either the measured degree of texture or the DP, to factors such as the Marsh score determined under light microscopy from tissue samples obtained by conventional endoscopy with biopsy. The reason for the lack of correlation between Marsh score and symptoms of celiac disease is currently unknown. The method described in this study, and in particular the texture analysis, may be helpful not only in diagnosis but also to clarify the relationship between Marsh score and symptoms with objective measures. Furthermore, it may be helpful to assess other diseases including inflammatory bowel disease.

4.4. *Limitations*

We used a limited set of retrospectively obtained videocapsule images. For validation, this analysis should be repeated in a prospective set of data from a larger group of patients, with inclusion of both exemplar and test data, so that the predictive value of the measurements is assessed. Based on the power test (see Section 2) significance could not be reached in comparing celiac versus control parameters at the five individual locations (N = 12 and 11, respectively). Use of a larger group of celiac and control patients and videoclips in a follow-up study will provide information regarding location-specific properties of textural and DP parameters. Videocapsule endoscopy was performed in the celiac patients after the start of a gluten free diet. Normalization of the mucosa may have begun, impacting image quantitation. Thus in future studies data should be

analyzed prior to commencement of the diet. Comparison of these results to measurements made with conventional endoscopic images [19] and with histology would assist in determining the merits of computer enhancement and quantitative analysis. Comparison of quantitative values in celiacs versus other patients such as those with Crohn's disease, NSAIDs damage, polyps, and tumors would be useful to determine the sensitivity and specificity of the method to detect celiac disease. Although significant results were presented in our study, alternative methods including computer vision and machine-learning methods can also be used as diagnostic tests for presence of intestinal lesions and motor disorders [20].

5. Conclusions

Our study confirms that the entire appearance of each videocapsule image was homogeneous for the control patients while heterogeneous in celiac patients despite the presence of artifacts. It was found that both the variability of textural properties and the variability of feature edges was significantly greater in celiacs as compared with controls, and that the magnitudes of these parameters were directly related to the DP, thus suggesting a relationship between small intestinal villous atrophy and gastrointestinal motility. Original images were transformed to a set of basis images with only salient information retained, prior to analysis. This enabled the complete elimination of the need for noise removal preprocessing steps, which is potentially important particularly when many image frames are analyzed and as the image resolution increases. The computerized frame-to-frame periodicity and the measure of textural-based quantitative changes in the videoclip series offers a potentially useful objective tool to distinguish controls from celiac patients. Since inter-observer variability in capsule interpretation can be significant, automatic image quantitation to assess disease state may be efficacious for improved diagnosis and treatment of celiac patients.

Conflict of interest statement

The authors have no conflicts of interest to report.

Acknowledgement

The implementation of this study was made possible in part with a grant from the Celiac Sprue Association Peer Review Research Grant Program.

REFERENCES

[1] P.H. Green, Mortality in celiac disease, intestinal inflammation, and gluten sensitivity, JAMA 302 (2009) 1225–1226.
[2] P. Brar, G.Y. Kwon, I.I. Egbuna, S. Holleran, R. Ramakrishnan, G. Bhagat, P.H. Green, Lack of correlation of degree of villous atrophy with severity of clinical presentation of coeliac disease, Dig. Liver Dis. 39 (2007) 26–29.
[3] P.H. Green, C. Cellier, Celiac disease, N. Engl. J. Med. 357 (2007) 1731–1743.
[4] E. Rondonotti, C. Spada, D. Cave, M. Pennazio, M.E. Riccioni, I. De Vitis, D. Schneider, T. Sprujevnik, F. Villa, J. Langelier, A. Arrigoni, G. Costamagna, R. de Franchis, Video capsule enteroscopy in the diagnosis of celiac disease: a multicenter study, Am. J. Gastroenterol. 102 (2007) 1624–1631.
[5] P.H. Green, Celiac disease: how many biopsies for diagnosis? Gastrointest. Endosc. 67 (2008) 1088–1090.
[6] M. Rewers, Epidemiology of celiac disease: what are the prevalence, incidence, and progression of celiac disease? Gastroenterology 128 (2005) S47–S51.
[7] A. Culliford, J. Daly, B. Diamond, et al., The value of wireless capsule endoscopy in patients with complicated celiac disease, Gastrointest. Endosc. 62 (2005) 55–61.
[8] R. Eliakim, Video capsule endoscopy of the small bowel, Curr. Opin. Gastroenterol. 26 (2010) 129–133.
[9] P.H. Green, M. Rubin, Capsule endoscopy in celiac disease: diagnosis and management, Gastrointest. Endosc. Clin. N. Am. 16 (2006) 307–316.
[10] Y.C. Metzger, S.N. Adler, A.B. Shitrit, B. Koslowsky, I. Bjarnason, Comparison of a new PillCam™ SB2 video capsule versus the standard PillCam™ SB for detection of small bowel disease, Rep. Med. Imag. 2 (2009) 7–11.
[11] C. Gheorghe, R. Iacob, I. Bancila, Olympus capsule endoscopy for small bowel examination, J. Gastrointest. Liver Dis. 16 (2007) 309–313.
[12] E.J. Ciaccio, A.B. Biviano, W. Whang, A.L. Wit, H. Garan, J. Coromilas, New methods for estimating local electrical activation rate during atrial fibrillation, Heart Rhythm 6 (2009) 21–32.
[13] E.J. Ciaccio, A.B. Biviano, W. Whang, A.L. Wit, J. Coromilas, H. Garan, Optimized measurement of activation rate at left atrial sites with complex fractionated electrograms during atrial fibrillation, J. Cardiovasc. Electrophysiol. 21 (2010) 133–143.
[14] E.J. Ciaccio, C.A. Tennyson, S.K. Lewis, S. Krishnareddy, G. Bhagat, P.H. Green, Distinguishing patients with celiac disease by quantitative analysis of videocapsule endoscopy images, Comput. Methods Programs Biomed. 100 (2010) 39–48.
[15] A.P. Berg, W.B. Mikhael, An efficient structure and algorithm for image representation using nonorthogonal basis images, IEEE Trans. Circ. Syst. II: Analog Digital Signal Process. 44 (1997) 818–828.
[16] E.J. Ciaccio, C.A. Tennyson, G. Bhagat, S.K. Lewis, P.H. Green, Classification of videocapsule endoscopy image patterns: comparative analysis between patients with celiac disease and normal individuals, Biomed. Eng. Online 9 (2010) 44–54.
[17] J.A. Murray, A. Rubio-Tapia, C.T. Van Dyke, D.L. Brogan, M.A. Knipschield, B. Lahr, A. Rumalla, A.R. Zinsmeister, C.J. Gostout, Mucosal atrophy in celiac disease: extent of involvement, correlation with clinical presentation, and response to treatment, Clin. Gastroenterol. Hepatol. 6 (2008) 186–193.
[18] P. Usai, G. Bassotti, P. Usai Satta, M. Cherchi, A. Plesa, F. Boy, A. Morelli, A. Balestrieri, Oesophageal motility in adult coeliac disease, Neurogastroenterol. Motil. 7 (1995) 239–244.
[19] E.J. Ciaccio, G. Bhagat, C.A. Tennyson, S.K. Lewis, L. Hernandez, P.H. Green, Quantitative assessment of endoscopic images for degree of villous atrophy in celiac disease, Dig. Dis. Sci. 56 (2011) 805–811.
[20] C. Malagelada, F. De Iorio, F. Azpiroz, A. Accarino, S. Segui, P. Radeva, J.R. Malagelada, New insight into intestinal motor function via noninvasive endoluminal image analysis, Gastroenterology 135 (2008) 1155–1162.